Research article

Analysis of cuproptosis-related genes in prognosis and immune infiltration in grade 4 diffuse gliomas

Hui Liu [a,1], Xin Bao [b,1], Zhirui Zeng [c,1], Wei Liu [d], Meifang Li [d,*]

[a] Department of Neurosurgery, Affiliated Hospital of Qingdao University, Qingdao, China
[b] School of Clinical Medicine, Guizhou Medical University, Guiyang, China
[c] School of Basic Medicine, Guizhou Medical University, Guiyang, China
[d] Department of Oncology, Changle County People's Hospital, Weifang, China

ARTICLE INFO

ABSTRACT

Background: Grade 4 diffuse gliomas are highly malignant tumours with poor prognosis. Cuproptosis is a novel form of cell death. Cuproptosis genes are associated with various tumours and affect the prognosis of patients with these tumours. However, the relationship between cuproptosis and grade 4 diffuse gliomas remains unclear.

Methods: Differentially expressed genes associated with cuproptosis in grade 4 diffuse gliomas were identified. Second, the prognostic model was established by univariate and multivariate COX regression analyses, and the genes ($p < 0.05$) were selected for subsequent analysis. The endpoint of the study was death. Single-gene analysis was performed in accordance with the expression levels of SLC31A1. Third, based on the expression levels of SLC31A1, gene function enrichment, drug sensitivity, and immune cell infiltration analyses were performed. Finally, the expression and biological functions of SLC31A1 in grade 4 diffuse gliomas were identified using immunohistochemical staining, qRT-PCR, and related biological experiments.

Results: We identified six coproptosis genes in the grade 4 diffuse gliomas dataset (SLC31A1, PDHA1, GLS, FDX1, LIPT1, and ATP7B). The six key cuproptosis genes of grade 4 diffuse gliomas were analysed using univariate COX analysis. Basic patient data, including age, race, year of diagnosis, sex, and treatment, were included in the univariate COX analysis. Then, multivariate COX analysis was performed for the factors with $p < 0.2$ in the univariate COX analysis. Age, year of diagnosis, and SLC31A1, PDHA1, and FDX1 levels were found to be independent prognostic factors. A nomogram was constructed using these 5 factors. Through experiments, we found that SLC31A1 had a higher expression level in cancer tissue than that near cancer among the three genes, SLC31A1, PDHA1, and FDX1; therefore, we focused on SLC31A1. According on the expression level of SLC31A1, we performed gene function enrichment, drug sensitivity, and immune cell infiltration analyses. Navitoclax was the most sensitive drug. Differential gene function enrichment was observed for metalloendopeptidase activity. SLC31A1 is expressed in dendritic cells, macrophages, neutrophils, and CD8+T cells. SLC31A1 is highly expressed in grade 4 diffuse gliomas, whereas SLC31A1 knockdown significantly reduces cell proliferation and mobility.

Conclusions: Age, year of diagnosis, and SLC31A1, PDHA1, and FDX1 expression were independent prognostic factors. A nomogram was constructed based on age, year of diagnosis, and SLC31A1, PDHA1, and FDX1 levels. Through analysis and experimental verification, SLC31A1

---

* Corresponding author.
  E-mail address: limeifang1001@163.com (M. Li).
[1] Equal contribution.

was found to affect the prognosis and progression of patients with grade 4 diffuse gliomas and was associated with immune cell infiltration.

1. Introduction

IDH wild-type grade 4 diffuse gliomas and grade 4 IDH mutant astrocytomas were renamed grade 4 diffuse gliomas in the 2021 WHO Classification of Central Nervous System Tumors [1]. Grade 4 diffuse gliomas are highly malignant and rapidly progress. Patients often exhibit symptoms of incremental intracranial stress, including headaches, and focal or developing neurological defects. Seizures occur in no < 25 % of patients and may appear later in the disease in up to 50 % of the patients [2]. Treatment of newly diagnosed grade 4 diffuse gliomas requires a multidisciplinary approach. The current standard of care consists of maximal secure surgical ectomy and consistent radiation therapy with temozolomide (TMZ, an oral alkylating chemotherapy agent) (Temodar®), followed by adjuvant chemotherapy with TMZ (National Comprehensive Cancer Network, 2015) [3]. Unfortunately, wide and total chirurgic operation for grade 4 diffuse gliomas is difficult because these tumours are frequently aggressive and located in the functional zones of the brain, including zones that control language, motor function, and sensation. Furthermore, because of its aggressive nature, radical resection of the primary tumour block cannot be cured, and infiltrating tumour cells are always retained around the brain, leading to subsequent disease progression or recurrence [4].

Copper deficiency disrupts the function of copper-conjunct enzymes, and copper accumulation leads to cell death [5]. Recently, it was discovered that copper, but not copper ionophores, is toxic to cells. Cuproptosis is a newly discovered type of cell death, which is different from other known forms of death, including apoptosis, iron production, and necrosis. It relies on mitochondrial respiration rather than adenosine triphosphate (ATP) production [6]. Studies have shown that cuproptosis is associated with the prognosis of bladder cancer and immune response [7]. Other studies have shown that cuproptosis genes are associated with low-grade gliomas [8]. According to other studies, the cuproptosis gene, FDX1, promote glioblastoma proliferation [9]. Studies have shown that the activation of cuproptosis in grade 4 diffuse gliomas can enhance the cytotoxic effect of regorafenib on tumour cells [10]. However, the characteristics of cuproptosis in the occurrence, evolution, and prognosis of grade 4 diffuse gliomas remain unclear.

Grade 4 diffuse gliomas are highly malignant, undergo incomplete resection, and are prone to recurrence. The tumour was highly treatment-resistant. This study analysed data from public databases to determine the relationship between cuproptosis and the prognosis of grade 4 diffuse gliomas, to identify drug targets for better treatment of grade 4 diffuse gliomas and improve patient prognosis.

2. Materials and methods

2.1. Data collection

Data were collected from the RNA sequencing expression profiles of 173 patients with grade 4 diffuse gliomas in the TCGA dataset (https://portal.gdc.cancer.gov/projects/TCGA-SKCM). Additionally, Tsvetkov et al. identified 12 genes associated with cuproptosis from previous literature (2022) [6] (Supplement Table 1). The validation set was a grade 4 diffuse gliomas RNA expression matrix obtained from the CGGA dataset (http://www.cgga.org.cn/). This study excluded seven patients with grade 4 diffuse gliomas with unknown survival and treatment information. Finally, survival data of 166 patients with this type of glioma were obtained. A flowchart is shown in Supplementary Fig. 1. The baseline clinical characteristics are shown in Table 1.

Table 1
Baseline clinicopathological features and treatments.

Variables	Number of patients
Age	166
<60	78
≥60	88
Race	166
White	148
Other	18
The year of diagnosis	166
<2008	80
≥2008	86
Living condition	166
Dead	135
Alive	31
Sex	166
Female	59
Male	107
Treatment	166
Surgery	150
Biopsy	16

2.2. Differential genes of the cancer genome atlas (TCGA) database

Differentially expressed genes (DEGs) in tissues from the two grade 4 diffuse gliomas groups in TCGA database (https://www. cancer.gov/about-nci/organization/ccg/research/structural-genomics/tcga) were examined using the Wilcoxon test method in R (R version 4.2.0) package 'limma'. Finally, we obtained the differential genes with p-value <0.05 (Supplement table 2). This analysis identified DEGs between tumour and paracancerous tissues.

2.3. The cuproptosis genes of grade 4 diffuse gliomas

The cuproptosis genes of grade 4 diffuse gliomas were identified by screening the differential genes in TCGA and the intersection of cuproptosis-related genes (Venn) obtained from the literature (Supplement table 3). The results of this process were obtained using R language. Subsequently, a model was constructed for prognosis and experimental verification.

2.4. The cuproptosis genes and clinical characteristics of grade 4 diffuse gliomas were used to construct a prediction model

First, the X-tile software was used to obtain the best cutoff values for each of the included factors. Second, the obtained cuproptosis genes and clinical characteristics were used to construct a Cox univariate proportional hazards model. Then, $p < 0.2$ cuproptosis genes were incorporated into a multifactor proportional risk model to obtain independent prognostic factors, and a nomogram was established using R package 'rms'. The endpoint of the study was death. Next, Kaplan-Meier (KM) survival curves were plotted using R package 'survminer'. If the survival curves evaluated by the log-rank test differed, a p-value <0.05 was considered statistically significant. Finally, R package 'survivalROC' was applied to create ROC curves. We also employed calibration curve, Concordance Index, and ROC curve (higher AUC [zone under ROC curve] values generally indicate higher forecast accuracy) to verify the accuracy demonstrated by the conjunct models. The horizontal axis of the calibration plot represents the forecasted survival rate, whereas the vertical axis represents the practical survival rate. The closer the predicted survival rate is to the real survival rate, the higher the overlap between the calibration curve and the reference line.

2.5. Prediction model construction and verification (CGGA and GEO)

Grade 4 diffuse gliomas data were obtained from the Chinese Glioma Genome Atlas (CGGA) (http://www. cgga. org. cn/) and Gene Expression Omnibus (GEO) (https://www.ncbi.nlm.nih.gov/geo/) (GSE16011) databases, and a clinical prediction model was constructed. The ROC curve verified the accuracy of the model. The ROC curve was obtained using R language.

2.6. Screening for differential genes and functional enrichment analysis of GO (gene ontology)

High and low expression of SLC31A1 genes were grouped, differential genes were screened, and a volcano map and heat map were generated. In addition, GO functional enrichment analyses were conducted on differentially expressed SLC31A1 genes.

2.7. Analysis of immune cell infiltration

Immune cell infiltration in patients with grade 4 diffuse gliomas was evaluated using the Tumour Immune Evaluation Resource (TIMER) website [11,12]. Correlation analysis was conducted using the tricarboxylic acid cycle and lipid metabolism genes.

2.8. Drug sensitivity analysis

The GSCA database (http://bioinfo.life.hust.edu.cn/web/GSCALite/) was used for drug sensitivity analysis. Consequently, sensitive drugs corresponding to each target gene were obtained. Through this process, sensitive drugs can be obtained for the treatment of diseases.

2.9. Analysis of SLC31A1 and Pan-Cancer

TIMER 2.0 (http://timer.cistrome.org/) analysis of SLC31A1 was undertaken for different tumour immune cell infiltration and expression levels. PrognoScan (http://dna00.bio.kyutech.ac.jp/PrognoScan/index.html) was employed to examine different tumour survival scenarios in the SLC31A1 high and low expression groups.

2.10. Cell culture and transfection

A normal neurogliocyte cell line (NHA) and three grade 4 diffuse glioma cell lines, U87, LN229, and LN18, were obtained from ATCC (USA). All of them were cultivated in DMEM medium (Servicebio, Beijing, China) containing 10 % foetal bovine serum (Hyclone, USA) in the cell incubation chamber with 5 % CO2 at 37 °C. NC and SLC31A1 short hairpin RNAs (shRNAs) were obtained from Sangon (Shanghai, China). shRNA transfection was performed using Polybrene (Sangon, Shanghai, China).

2.11. qRT-PCR

Whole RNA from NHA, U87, LN229, and LN18 cells was obtained using TRIzol reagent. SuperScript IV reverse transcription reagent (Thermo Fisher Scientific, USA) was used to conduct reverse transcription. A total of 200 ng of cDNA from each sample was used for PCR amplification and real-time monitoring using the SYBR green reagent (Yeasen, Shanghai, China). SLC31A1 expression was normalized to β-actin. The primers used in the current research were exhibited as follows: SLC31A1 forward primer, 5′-GGGGAT-GAGCTATATGGACTCC-3′; SLC31A1 reverse primer, 5′-TCACCAAACCGGAAAACAGTAG-3′; β-actin forward primer, 5′-CATG-TACGTTGCTATCCAGGC-3′; β-actin reverse primer, and 5′-CTCCTTAATGTCACGCACGAT-3′.

2.12. Immunohistochemical (IHC) staining

A total of 26 pairs of grade 4 diffuse glioma tissues and contiguous non-tumour tissues were acquired from the Affiliated Hospital of Qingdao University, with the approval of the Medical Ethics Committee of the Affiliated Hospital of Qingdao University. The patients in this study did not receive adjuvant therapy, neoadjuvant therapy, or radiotherapy before tissue collection. Written informed consent was obtained from all the patients. For IHC, tissues were chopped into 2 μm sections, then de-paraffinised and rehydrated in xylene and ethanol. The tissues were then incubated in citrate buffer for 10 min and placed in a high-temperature, high-pressure environment for antigen retrieval. Endogenous peroxidase activity and nonspecific antigens in the sections were blocked with 3 % H_2O_2 and 5 % BSA (Boster, Beijing, China). Anti-SLC31A1 monoclonal antibody (1:1000; Cat no. 67221-1-Ig, Proteintech, Wuhan, China) was appended for sections overnight at 4 °C. After treatment with the secondary antibody, an antigen-antibody complex was developed using DAB.

2.13. Cell prolfieration detection

Cell proliferation was detected using the CCK-8 and EDU assays. For the CCK-8 assay, cells were seeded at a density of 3×10^3 cells/well in a 96-well plate, with each group comprising six replicates. Subsequently, 10 μl of CCK-8 reagent (Shanghai Univ Biological Technology, Ltd.) was injected into each well at 24, 48, 72, and 96 h. The absorbance of PC cells in each well was measured at 450 nm using an automatic enzyme label detector (Thermo Fisher Scientific). For EDU assay, it was performed based on BeyoClick™ EdU-488 kit (Beyotime, China) according to the instructions provided by the manufacturer.

2.14. Cell mobility detection

Wound healing and transwell assays were used to detect cell mobility. For the wound healing assay, cells were introduced into 6-well plates and allowed to grow until they reached 90 % confluence. After the creation of an artificial wound in a single layer of cells, medium containing 1 % FBS was replaced. After a period of 24 h, wound closure was documented to determine the percentage of wound healing. For transwell assay, a suspension of 200 μL (containing 2.0×10^4 cells) and 500 μL of medium containing 10 % FBS were introduced into the upper (precoated with matrigel) and lower compartments of a Transwell chamber (Millipore, Billerica, MA, USA), respectively. After 24 h, fixed cells in the lower compartment were stained with crystal violet for 20 min. The migratory cell count was subsequently determined by randomly selecting and counting cells in five fields from each sample.
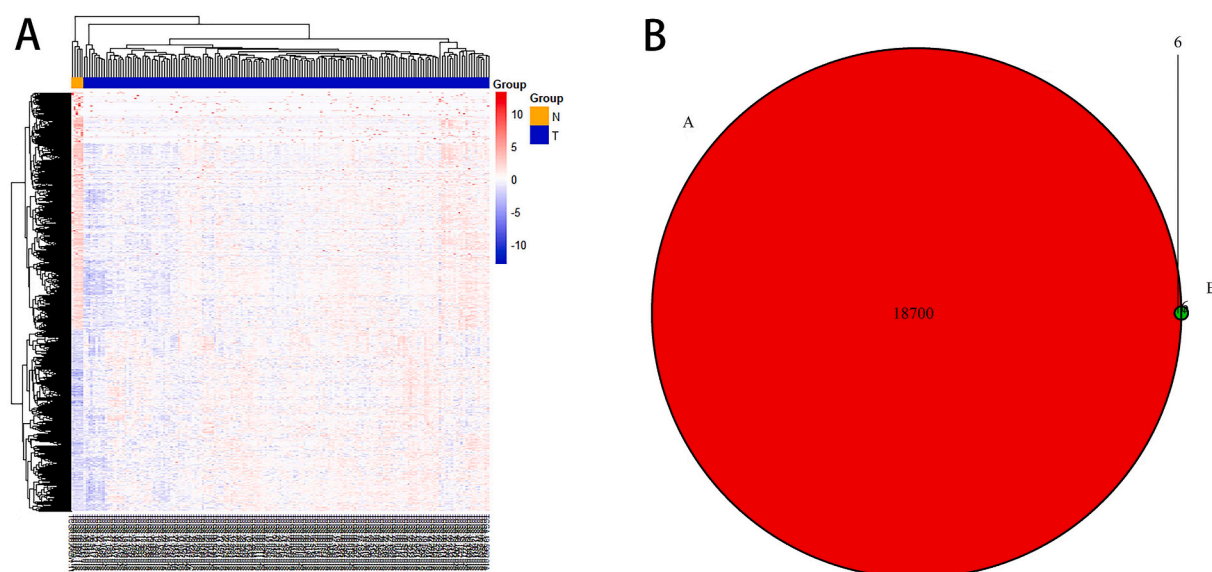

Fig. 1. Differentially expressed genes analysis heatmap of grade 4 gliomas in TCGA Database (A) and venn map of cuproptosis gene (B).

2.15. Data statistics

The results were analysed using SPSS 20.0. An unpaired *t*-test was used to analyse the differences between two groups, whereas one-way analysis of variance was used to analyse the differences between multiple groups. *P*-value <0.05 was set as cut-off. R software v4.2.0 (R Foundation for Statistical Computing, Vienna, Austria) was used for statistical analyses. Fisher's exact test or Pearson's chi-square test was used to analyse qualitative variables. Quantitative variables were analysed using the nonparametric Wilcoxon rank-sum test (for unpaired samples). The Kruskal–Wallis test was used to normalise multiple groups.

3. Results

3.1. Differential genes were filtrated from TCGA database, and cuproptosis genes were screened from TCGA database

The data of 173 patients with grade 4 diffuse glioma were obtained from TCGA database. Patients with unknown survival and treatment information were excluded. Finally, 166 patients with grade 4 diffuse gliomas were identified. The R language 'limma' package was used to compare the differential genes between the paracancerous tissues and tumour. Differential genes were screened using $|\log2FC| > 0$ and $p < 0.05$ (Fig. 1A); six cuproptosis genes in this grade 4 diffuse glioma dataset (SLC31A1, PDHA1, GLS, FDX1, LIPT1, and ATP7B) were obtained by intersection with known cuproptosis genes (Fig. 1B).

3.2. COX proportional hazards model and nomogram prediction model were established for the 6 cuproptosis genes obtained, and the clinical data were collected from TCGA dataset

First, we used the X-tile software to obtain the best cutoff values for each of the included factors. Second, univariate Cox regression analysis was performed on age, year of diagnosis, sex, race, treatment measures, and six cuproptosis genes in TCGA dataset. Third, variables with p-values <0.2 (age, year of diagnosis, SLC31A1, PDHA1, GLS, FDX1, and LIPT1) were included in the multivariate COX regression analysis. Multivariate Cox regression analysis ($p < 0.05$) of variables (age, year of diagnosis, SLC31A1, PDHA1, and FDX1) was used to establish a nomogram. K-M analysis of age, year of diagnosis, and SLC31A1, PDHA1, and FDX1 expression was performed. Finally, the C-index and AUC zones under the ROC curve of the pattern were figured to verify the accuracy and precision of the model (Fig. 2A–K). The AUC at 12, 24, and 36 months were 0.676, 0.751, and 0.764, respectively.
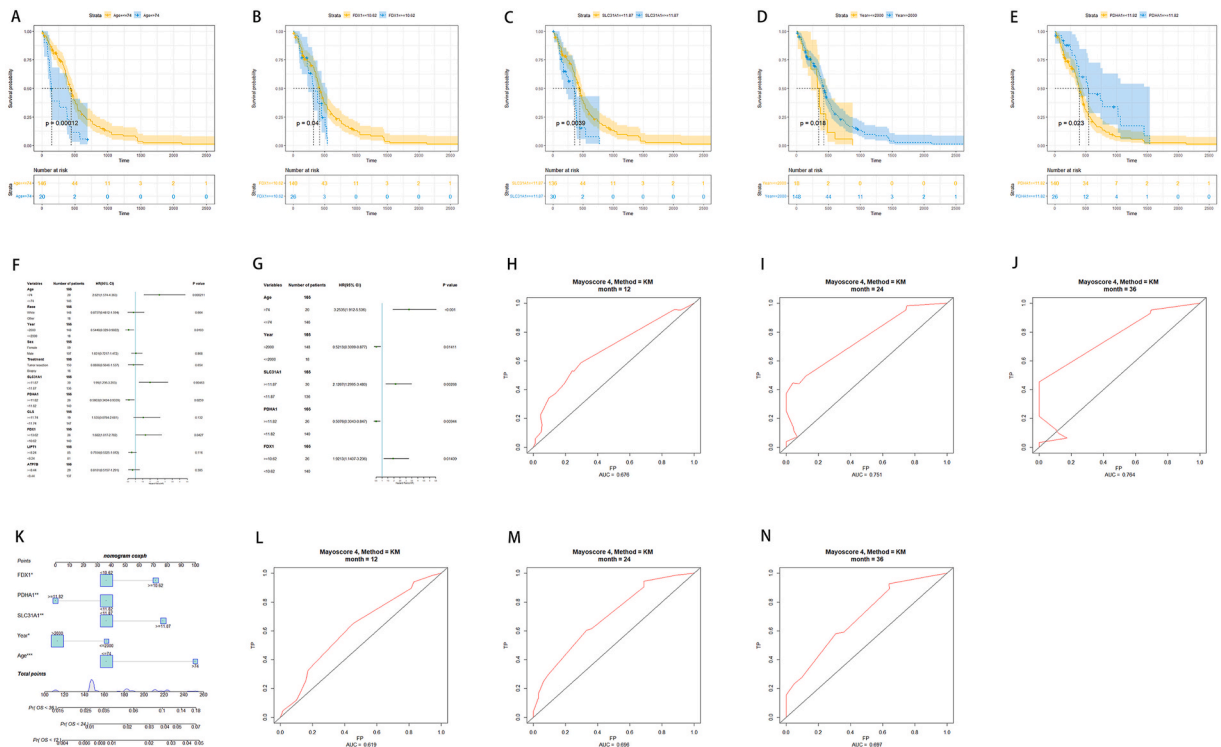

Fig. 2. The building process of the prognostic signature. Kaplan-Meier survival analysis (A–E) and univariate and multivariate COX regression analysis (F, G) for patients of Grade 4 gliomas in TCGA Database. The time-dependent ROC analysis of 1-year, 2-year, and 3-year OS (H–J) for patients of grade 4 gliomas in TCGA Database. Establish a nomogram of independent prognostic factors (K). The time-dependent ROC analysis of 1-year, 2-year, and 3-year OS (L–N) for patients of Grade 4 gliomas in CGGA Database. Year represents the year of diagnosis.

3.3. The grade 4 diffuse gliomas data were screened from CGGA database and GEO database to establish the model of TCGA database data for external verification

Data on grade 4 diffuse gliomas were obtained from CGGA and GEO databases, and a clinical prediction model was constructed. ROC curve (Fig. 2L-N) was used to calculate AUC to verify the model's accuracy. After analysis, the AUC at 12, 24, and 36 months were 0.619, 0.696, and 0.697, respectively, in the CGGA database. In the GEO database, the AUC at 12, 24, and 36 months were 0.71, 0.77, and 0.85, respectively (Supplement Fig. 2). The results indicated that the reliability of the model was relatively high.
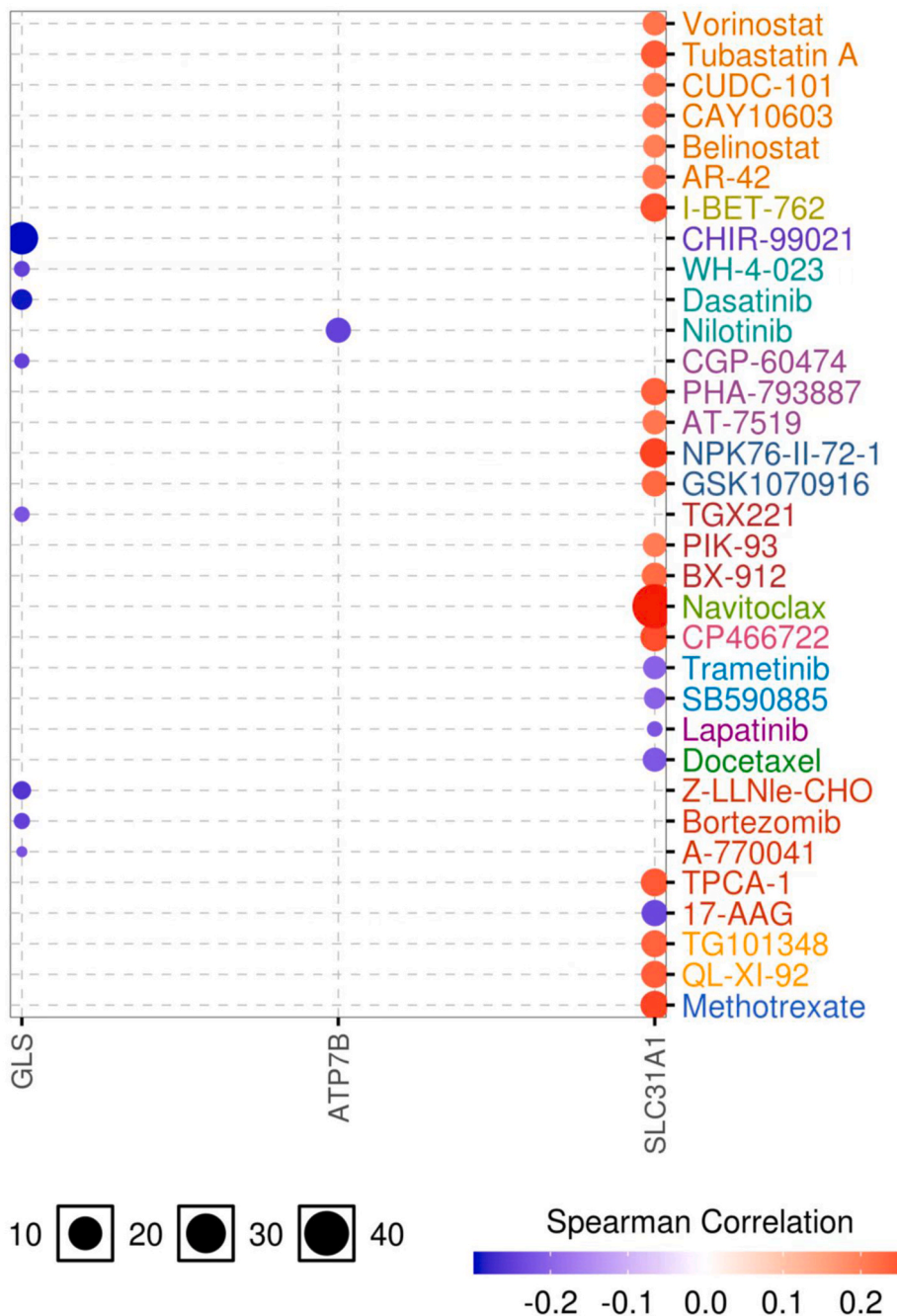

Fig. 3. Drug susceptibility analysis of three genes.

3.4. Drug sensitivity analysis

The GSCA database (http://bioinfo.life.hust.edu.cn/web/GSCALite/) was used for the drug susceptibility analyses. The cells were also sensitive to Navitoclax, Methotrexate, and Vorinostat (Fig. 3). Next, we selected SLC31A1 for single-gene analysis.

3.5. SLC31A1 gene expression level was grouped, and differential genes were screened. GO functional enrichment analysis were executed

High and low expression of the SLC31A1 gene were grouped, the differential genes were screened, and a heat map (Fig. 4A) and volcano map (Fig. 4B) were created for display. Finally, GO functional enrichment analyses (Fig. 4C and D) were performed for DEGs. The ROC curve of the model was constructed with SLC31A1 gene (Fig. 4E–G).

3.6. Analysis of immune cell infiltration

Immune cell infiltration in patients with grade 4 diffuse gliomas was evaluated using the Tumour Immune Evaluation Resource (TIMER) website. According to the literature, PD-1 is related to CD8+T, TP53, ATM, and POLE, which are the target genes of PD-1. Hence, we performed the correlation analysis of SLC31A1 and TP53, ATM, and POLE and found a certain correlation (Fig. 5A). SLC31A1 was associated with CD8$^+$ T cells, macrophages, neutrophils, and dendritic cells (Fig. 5B). In addition, a correlation analysis was conducted with genes related to the tricarboxylic acid cycle (IDH1) and lipid metabolism (ALDOC and FH) (Fig. 5C). The results revealed that SLC31A1 was positively correlated with IDH1 and FH and negatively correlated with ALDOC.

3.7. Analysis of SLC31A1 and Pan-Cancer

SLC31A1 analysis was performed under different tumour immune cell infiltration conditions, and the amount of expression in different tumours was determined using TIMER2.0 (http://timer.cistrome.org/) in the TCGA database (Supplement Figs. 3A–D). Furthermore, SLC31A1 high- and low-expression groups were analysed for different tumour survival situations using PrognoScan (http://dna00.bio.kyutech.ac.jp/PrognoScan/index.html) (Fig. 6A-M).

3.8. SLC31A1 was highly expressed in grade 4 diffuse gliomas, while knockdown of SLC31A1 reduced cell proliferation and mobility

We first detected the mRNA level of SLC31A1 in glioma cell lines, including U87, LN229, and LN18, and the normal neurogliocyte line, NHA, using qRT-PCR. It was demonstrated that mRNA levels of SLC31A1 were higher in U87, LN229, and LN18 cells than in NHA cells (Fig. 7A). The protein expression of SLC31A1 was then detected by IHC in grade 4 diffuse glioma tissues and adjacent tissues. It was discovered that expression of SLC31A1 was significantly elevated in grade 4 diffuse glioma tissues (Fig. 7B–C). To determine the biological functions of SLC31A1, shRNA was used to inhibited the expression of SLC31A1 in U87 and LN229 cells (Fig. 7D–E). CCK-8
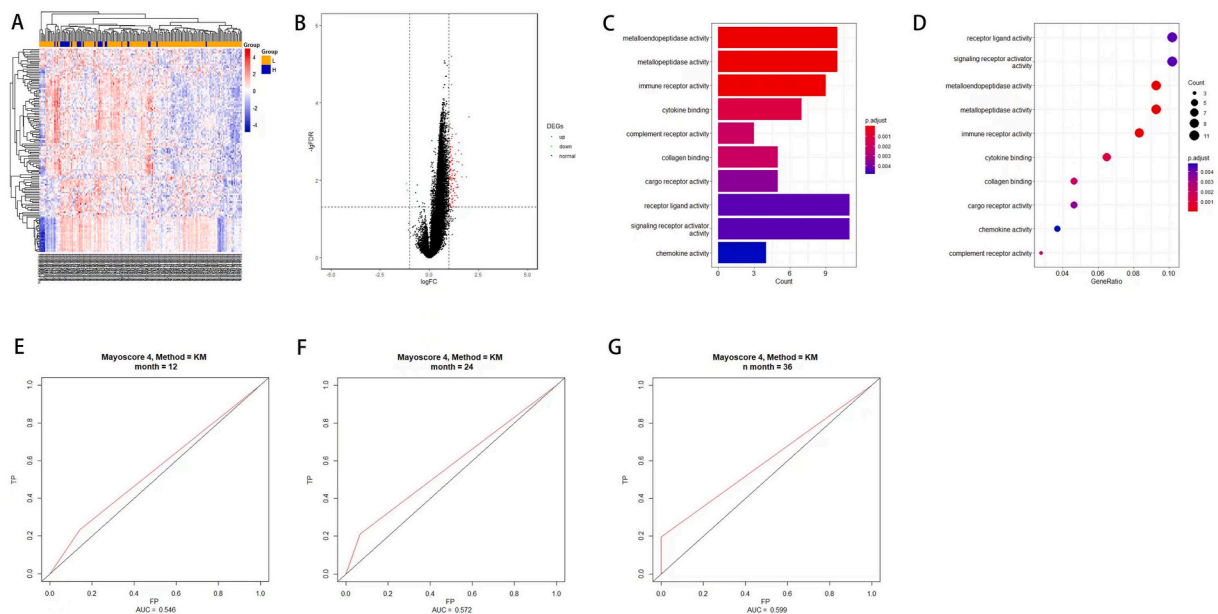

Fig. 4. The heatmap (A) and volcano map (B) of SLC31A1 were made. Gene function enrichment analysis by GO (Gene Ontology) was performed for differential genes (C, D). The time-dependent ROC analysis of 1-year, 2-year, and 3-year OS (E–G) of SLC31A1 for patients of Grade 4 gliomas in TCGA Database.
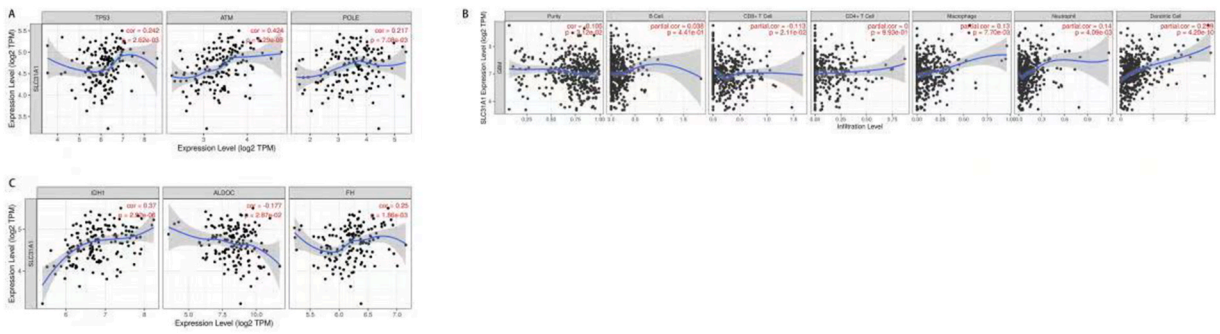
Fig. 5. Correlation of SLC31A1 with PD1 (A), immune cells (B) and metabolism (C).
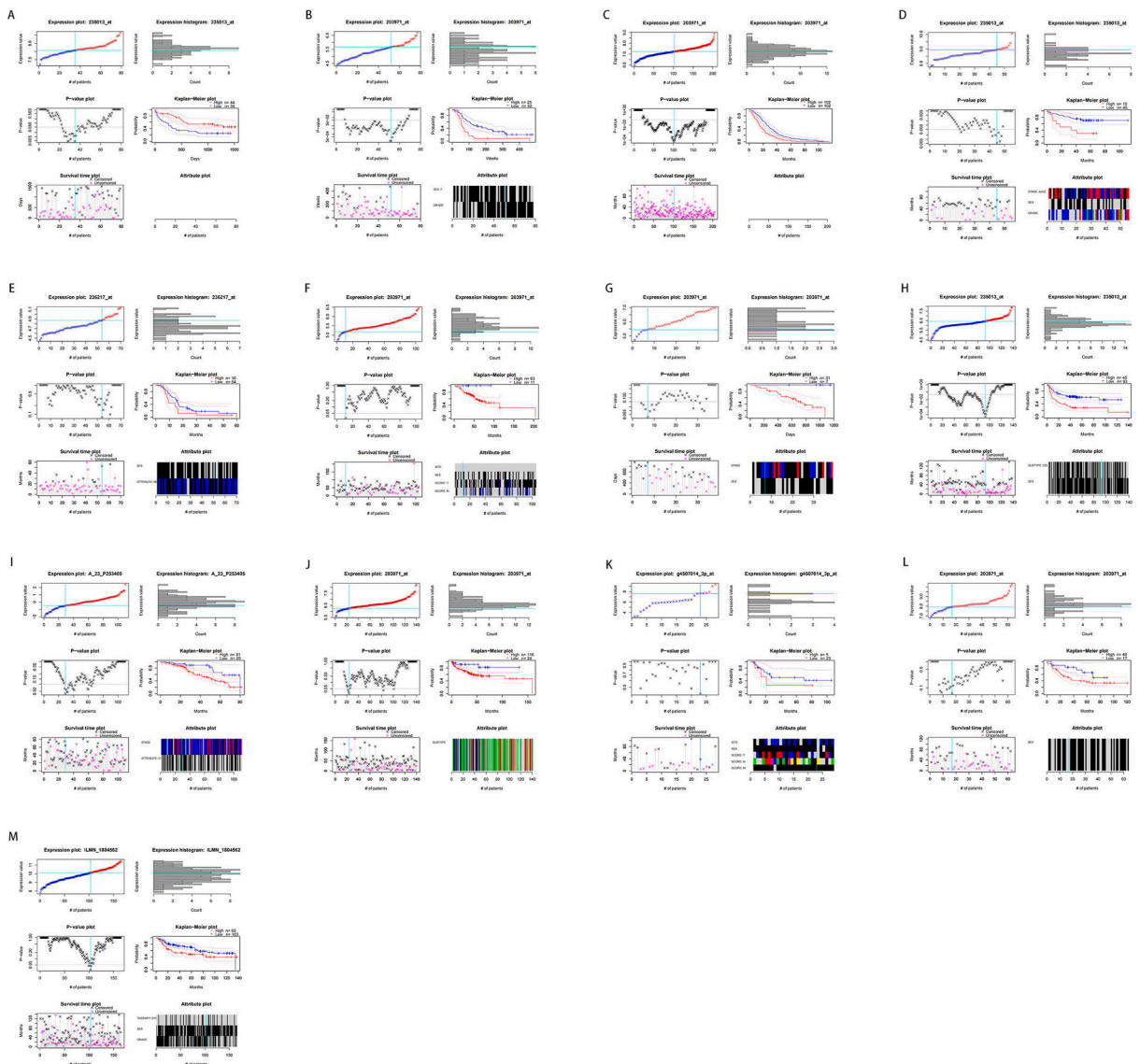

Fig. 6. Analysis of SLC31A1 and Pan-Cancer. (A) AML (acute myelocytic leukemia) (B) Astrocytoma (C) BRCA (Breast Cancer) (D) Colorectal cancer (E) GBM (Glioblastoma) (G) Melanoma (H) NSCLC (nonsmall-cell lung cancer) (I) Ovarian cancer (J) Soft tissue cancer Liposarcoma (K) Squamous cell carcinoma (L) Uveal melanoma (M) Bladder cancer.

(Fig. 7F) and EDU assays (Fig. 7G) indicated that SLC31A1 knockdown significantly reduced cell proliferation. Moreover, the SLC31A1 knockdown reduced cell migration (Fig. 7H) and invasion (Fig. 7I). Taken together, these results indicate that SLC31A1 is a novel oncogene in grade 4 diffuse gliomas.

4. Discussion

Grade 4 diffuse gliomas are the most frequent malignant tumours of the brain, but their mechanisms remain unclear. Currently, the treatment is surgical resection combined with radiotherapy and chemotherapy. However, its effects remain unclear. Cuproptosis is the most recent mode of death and has been discovered in various tumours [13–16]. Studies have shown that cuproptosis is associated with the prognosis of glioma [17]. Other studies have shown that cuproptosis may support chemotherapy and immunotherapy for glioblastoma [18]. It has been reported that the cuproptosis gene is associated with the prognosis of triple-negative breast cancer [19]. In addition, it has been found that grade 4 diffuse gliomas are related to iron death, metabolism, and apoptosis [20–22]. However, the relationship between cuproptosis and grade 4 diffuse gliomas remains unclear. This study aimed to investigate the relationship between cutaneous proptosis and the prognosis of grade 4 diffuse gliomas to provide a better treatment plan for grade 4 diffuse gliomas.

After screening, we identified six cuproptosis genes (SLC31A1, PDHA1, GLS, FDX1, LIPT1, and ATP7B) in grade 4 diffuse gliomas. FDX1 and lipoylation are key factors involved in copper ionophore–induced cell death. Excess copper promotes the aggregation and
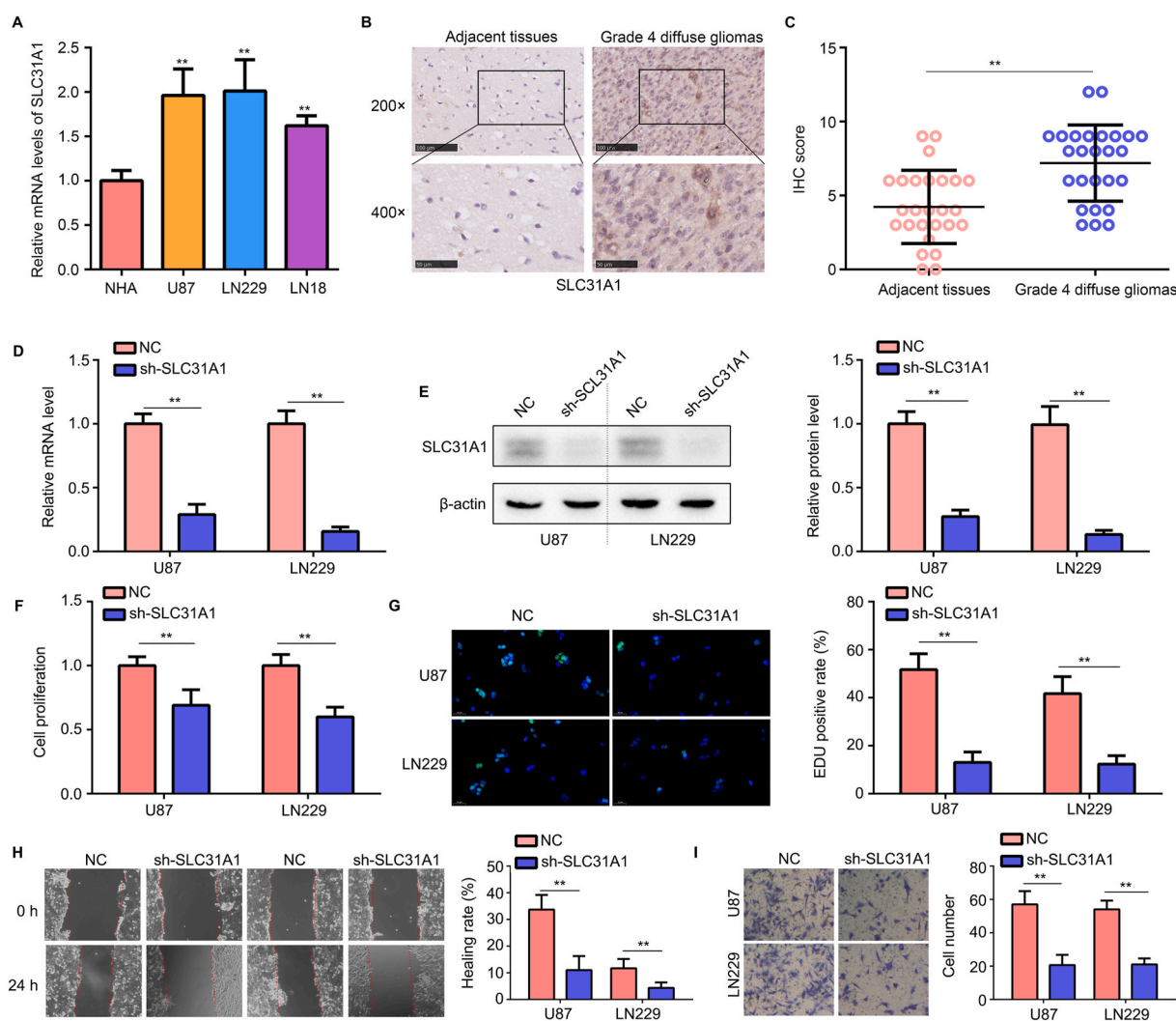

Fig. 7. Expression of SLC31A1 in glioma cell lines and tissues. (A) The mRNA level of SLC31A1 in glioma cell lines including U87, LN229 and LN18 and normal neurogliocyte line NHA via qRT-PCR. (B, C) Using IHC to detect the protein expression of SLC31A1 in grade 4 diffuse gliomas tissues and paracancerous tissues. (D–E) Targeting shRNA for SLC31A1 was used to construct SLC31A1 low expressed cells. The uncropped version of Fig. 7E as Supplement Fig. 4 has been provided. (F–G) CCK-8 and EDU assay were used to determine the effects of SLC31A1 on cell proliferation. (H–I) Wound healing assay and transwell assay were used to detect the effects of SLC31A1 on cell migration and invasion.

loss of function of lipoylated proteins, destabilising iron-sulfur clusters, leading to proteotoxic stress, and finally, cell death. FDX1 is an upstream regulator of lipoylation. Loss of FDX1 leads to complete loss of protein lipoylation, amassing of pyruvate and α-ketoglutarate, and consumption of succinate, indicating that loss of protein lipoylation blocks the tricarboxylic acid cycle (TCA) [6]. Copper is mainly absorbed by the transmembrane copper transporter SLC31A1 (also known as CTR1) and subsequently transmitted by a copper chaperone from superoxide dismutase (CCS) to SOD1, which plays an antioxidant role [23,24]. Pyruvate dehydrogenase E1 element sigma subunit α (PDHA1) is a crucial element of pyruvate dehydrogenase (PDH) complex (PDC), which is essential for glucose metabolism and is involved in oxidative phosphorylation and the tricarboxylic acid cycle in mitochondria [25]. PDC activity is adjusted by PDH kinase 4 (PDK1-4) at three autocephalous serine (Ser, S) residues: S293, S300, and S232 [26]. The inactivation of PDHA1 accelerates tumour glycolysis by downregulating PDC activity [27]. GLS and GLS2 have different configurable and kinetic features that contribute to their function and regulation. GLS displays oncogenic characteristics, and GLS2 has been confirmed as a tumour suppressor. Alternative genomic and epigenomic interventions in GLS function influence metabolic reprogramming in cancer [28,29]. Mutations in the ATP7A and ATP7B genes were validated to give rise to Menke's disease and Wilson's disease, respectively, which are characterised by the blockade and amassing of copper [30]. This study demonstrates that LIPT1 expression is inversely related to Treg infiltration. Thus, LIPT1 upregulation improves reactivity to immunotherapy by restraining Treg infiltration in the tumour microenvironment. Our study found that LIPT1-upregulated genes were enriched in several immune response–related pathways, including γ-IFN signalling. Thus, LIPT1 may ameliorate the curative effect of immunotherapy for the complete activation of γ-IFN signalling [31].

Gene ontology analysis revealed that the differentially expressed genes were enriched in metalloendopeptidase, metallopeptidase, and immune receptor activities by gene ontology analysis. This is consistent with our findings. The next step was to further investigate the specific mechanisms of the metalloendopeptidases.

Based on the expression level of SLC31A1, K-M analysis indicated that the survival rate of the high-expression group was lower than that of the low-expression group. This indicates that the expression of SLC31A1 is inversely proportional to the patient survival rate. Therefore, more research can be done around SLC31A1.

Immune cells are essential components of the tumour microenvironment and are valuable for predicting tumour prognosis [32]. Immune cell infiltration analysis of SLC31A1 showed that CD8+T cells, neutrophils, dendritic cells, and macrophages infiltrated to different degrees. According to the literature, PD-1 is related to CD8+T. cells, and we conducted a correlation analysis between SLC31A1 and PD-1 target genes (TP53, ATM, and POLE) and found that SLC31A1 correlated with them. According to literature, cuproptosis is related to the tricarboxylic acid cycle and lipid metabolism. Correlation analysis revealed that SLC31A1 was related to the target genes of the tricarboxylic acid cycle (IDH1) and lipid metabolism (ALDOC and FH). At last, Navitoclax, Methotrexate, and vorinostat were found to be sensitive to the SLC31A1 gene.

It is commonly acknowledged that glioma encompasses both lower-grade glioma (LGG) and glioblastoma (GBM), yet there exist significant disparities in their biological attributes, genomic profiles, and prognoses. As a result, our focus is squarely on the cuproptosis-related signature in Grade 4 diffuse gliomas, also known as GBM, which is not a replication of the work conducted by Zhang, Zihao et al. [33] who primarily investigated lower-grade glioma. Similarly, Wang, Jun et al. [34] examined gliomas in general, a scope we believe may lack precision. Drawing from the TCGA database, our analysis revealed that the level of SLC31A1 is notably elevated in GBM compared to LGG. Therefore, when assessing the prognostic impact of SLC31A1 in gliomas overall, there exists a bias due to the disparities in pathological features, given that survival rates among GBM patients are significantly lower than those with LGG. Therefore, compared with the research from Wang, Jun et al. research from our study was more precision. Moreover, in prior research conducted by Erliang Li et al. [35] and Zhang, Zihao et al. [36], a set of cuproptosis genes including FDX1, LIAS, LIPT1, DLD, DLAT, PDHA1, PDHB, MTF1, GLS, and CDKN2A were utilized. However, our study expanded upon this foundation, incorporating SLC31A1 and ATP7B into our analysis. This expansion reflects the ongoing scientific discovery of additional cuproptosis genes, enabling us to conduct a more comprehensive and contemporary examination. Taken together, our findings suggest that SLC31A1 may hold promise as a therapeutic target for Grade 4 diffuse gliomas, potentially guiding clinicians in selecting appropriate treatment strategies based on the expression levels of this gene.

This study highlights its strengths through a novel investigation of cuproptosis in grade 4 diffuse gliomas, the use of comprehensive bioinformatics and experimental approaches, and the identification of potential therapeutic targets. However, the study also has limitations, such as retrospective studies, potential biases in public datasets, limitations of the experimental validation methods, clinical information loss, and the need for prospective clinical trials to validate the findings. Finally, acknowledging the complexity of translating genomic and molecular findings into clinical practice is prudent, given the multifactorial nature of cancer progression and treatment response. As for the sensitivity analysis, there were few shedding data in this study (seven cases, 4.2 %), considering the low shedding rate (<5 %) and the possibility of random shedding. Therefore, we believe that shed data have little impact on this study; therefore, a missing value analysis cannot be performed. This study provides guidelines for the treatment of grade 4 diffuse gliomas. However, this tumour is highly malignant and has a low survival rate, requiring further investigation.

Lastly, SLC31A1 is an independent prognostic gene and is associated with immune cell infiltration in grade 4 diffuse gliomas.

5. Conclusions

The cuproptosis gene influences the prognosis of patients with grade 4 diffuse gliomas and is associated with immune cell infiltration. Five variables (age, year of diagnosis, and expression of SLC31A1, PDHA1, and FDX1) were included in the nomogram. The nomogram can predict the survival of patients with grade 4 diffuse gliomas. Immune cell infiltration analysis of SLC31A1 showed that CD8+T cells, neutrophils, dendritic cells, and macrophages infiltrated to different degrees. SLC31A1 gene has been confirmed as a

novel oncogene in grade 4 diffuse gliomas.

Ethics approval and consent to participate

Review and/or approval by an ethics committee was not needed for this study because the data used in this study are from public databases including TCGA database (https://portal.gdc.cancer.gov/projects/TCGA-SKCM), CGGA database (http://www.cgga.org.cn/) and GEO database (https://www.ncbi.nlm.nih.gov/geo/).

Consent for publication

This article agrees to be published.

Funding

Availability of data and materials

The data used in this paper are respectively from TCGA database (https://portal.gdc.cancer.gov/projects/TCGA-SKCM), CGGA database (http://www.cgga.org.cn/), and GEO database (https://www.ncbi.nlm.nih.gov/geo/) (GSE16011), all of which are public databases. Because it does not have its own data, it is not deposited into a publicly available repository.

CRediT authorship contribution statement

Hui Liu: Writing – original draft. **Xin Bao:** Data curation. **Zhirui Zeng:** Writing – review & editing, Data curation. **Wei Liu:** Data curation. **Meifang Li:** Writing – review & editing.

Declaration of competing interest

The authors declare the following financial interests/personal relationships which may be considered as potential competing interests:Meifang Li reports statistical analysis and writing assistance were provided by The Affiliated Hospital of Qingdao University. Hui Liu reports a relationship with The Affiliated Hospital of Qingdao University that includes: board membership and non-financial support. Meifang Li has patent pending to Hui Liu. The co-author has never worked as an editor in the journal. If there are other authors, they declare that they have no known competing financial interests or personal relationships that could have appeared to influence the work reported in this paper.

Acknowledgements

Appendix A. Supplementary data

Supplementary data to this article can be found online at https://doi.org/10.1016/j.heliyon.2024.e29212.

References

[1] D.N. Louis, et al., The 2021 WHO Classification of tumors of the Central nervous system: a summary, Neuro Oncol. 23 (8) (2021) 1231–1251.
[2] J. Perry, et al., The use of prophylactic anticonvulsants in patients with brain tumours-a systematic review, Curr. Oncol. 13 (6) (2006) 222–229.
[3] L.B. Nabors, et al., Central nervous system cancers, version 1.2015, J. Natl. Compr. Cancer Netw. 13 (10) (2015) 1191–1202.
[4] T.A. Wilson, M.A. Karajannis, D.H. Harter, Glioblastoma multiforme: state of the art and future therapeutics, Surg. Neurol. Int. 5 (2014) 64.
[5] M.A. Kahlson, S.J. Dixon, Copper-induced cell death, Science 375 (6586) (2022) 1231–1232.
[6] P. Tsvetkov, et al., Copper induces cell death by targeting lipoylated TCA cycle proteins, Science 375 (6586) (2022) 1254–1261.
[7] Q. Song, et al., Cuproptosis scoring system to predict the clinical outcome and immune response in bladder cancer, Front. Immunol. 13 (2022) 958368.
[8] J.H. Bao, et al., Identification of a novel cuproptosis-related gene signature and integrative analyses in patients with lower-grade gliomas, Front. Immunol. 13 (2022) 933973.
[9] M. Zhang, et al., A novel cuproptosis-related gene signature to predict prognosis in Glioma, BMC Cancer 23 (1) (2023) 237.
[10] W. Jia, et al., Brain-targeted HFn-Cu-rego nanoplatform for site-specific delivery and manipulation of autophagy and cuproptosis in glioblastoma, Small 19 (2) (2023) e2205354.
[11] T. Li, et al., TIMER: a web server for comprehensive analysis of tumor-infiltrating immune cells, Cancer Res. 77 (21) (2017) e108–e110.
[12] B. Chen, et al., Profiling tumor infiltrating immune cells with CIBERSORT, Methods Mol. Biol. 1711 (2018) 243–259.
[13] Z. Zhu, et al., A novel cuproptosis-related molecular pattern and its tumor microenvironment characterization in colorectal cancer, Front. Immunol. 13 (2022) 940774.

[14] J. Wang, et al., Identification of cuproptosis-related subtypes, construction of a prognosis model, and tumor microenvironment landscape in gastric cancer, Front. Immunol. 13 (2022) 1056932.

[15] Z. Liu, et al., Construction of cuproptosis-related gene signature to predict the prognosis and immunotherapy efficacy of patients with bladder cancer through bioinformatics analysis and experimental validation, Front. Genet. 13 (2022) 1074981.

[16] Y. Liu, et al., Role of cuproptosis-related gene in lung adenocarcinoma, Front. Oncol. 12 (2022) 1080985.

[17] W. Wang, et al., The cuproptosis-related signature associated with the tumor environment and prognosis of patients with glioma, Front. Immunol. 13 (2022) 998236.

[18] Y. Zhou, et al., EREG is the core onco-immunological biomarker of cuproptosis and mediates the cross-talk between VEGF and CD99 signaling in glioblastoma, J. Transl. Med. 21 (1) (2023) 28.

[19] S. Sha, et al., Prognostic analysis of cuproptosis-related gene in triple-negative breast cancer, Front. Immunol. 13 (2022) 922780.

[20] D. Xiao, et al., A ferroptosis-related prognostic risk score model to predict clinical significance and immunogenic characteristics in glioblastoma multiforme, Oxid. Med. Cell. Longev. 2021 (2021) 9107857.

[21] K.A. El, et al., Metabolic rewiring in glioblastoma cancer: EGFR, IDH and beyond, Front. Oncol. 12 (2022) 901951.

[22] N.C. Lucki, et al., A cell type-selective apoptosis-inducing small molecule for the treatment of brain cancer, Proc. Natl. Acad. Sci. U.S.A. 116 (13) (2019) 6435–6440.

[23] B. Zhou, J. Gitschier, hCTR1: a human gene for copper uptake identified by complementation in yeast, Proc. Natl. Acad. Sci. U.S.A. 94 (14) (1997) 7481–7486.

[24] V.C. Culotta, et al., The copper chaperone for superoxide dismutase, J. Biol. Chem. 272 (38) (1997) 23469–23472.

[25] M.S. Patel, et al., The pyruvate dehydrogenase complexes: structure-based function and regulation, J. Biol. Chem. 289 (24) (2014) 16615–16623.

[26] E. Kolobova, et al., Regulation of pyruvate dehydrogenase activity through phosphorylation at multiple sites, Biochem. J. 358 (Pt 1) (2001) 69–77.

[27] L. Yu, et al., The glycolytic switch in tumors: how many players are involved? J. Cancer 8 (17) (2017) 3430–3440.

[28] W.P. Katt, M.J. Lukey, R.A. Cerione, A tale of two glutaminases: homologous enzymes with distinct roles in tumorigenesis, Future Med. Chem. 9 (2) (2017) 223–243.

[29] J.M. Matés, J.A. Campos-Sandoval, J. Márquez, Glutaminase isoenzymes in the metabolic therapy of cancer, Biochim. Biophys. Acta Rev. Canc 1870 (2) (2018) 158–164.

[30] T. Nevitt, H. Ohrvik, D.J. Thiele, Charting the travels of copper in eukaryotes from yeast to mammals, Biochim. Biophys. Acta 1823 (9) (2012) 1580–1593.

[31] H. Lv, et al., Comprehensive analysis of cuproptosis-related genes in immune infiltration and prognosis in melanoma, Front. Pharmacol. 13 (2022) 930041.

[32] A.J. Gentles, et al., The prognostic landscape of genes and infiltrating immune cells across human cancers, Nat. Med. 21 (8) (2015) 938–945.

[33] Z. Zhang, et al., Cuproptosis-related gene signature stratifies lower-grade glioma patients and predicts immune characteristics, Front. Genet. 13 (2022) 1036460.

[34] J. Wang, et al., Cuproptosis-related gene SLC31A1 expression correlates with the prognosis and tumor immune microenvironment in glioma, Funct. Integr. Genomics 23 (3) (2023) 279.

[35] E. Li, et al., Cuproptosis-related gene expression is associated with immune infiltration and CD47/CD24 expression in glioblastoma, and a risk score based on these genes can predict the survival and prognosis of patients, Front. Oncol. 13 (2023) 1011476.

[36] Z. Zhang, et al., Cuproptosis-related gene signature stratifies lower-grade glioma patients and predicts immune characteristics, Front. Genet. 13 (2022) 1036460.

Abbreviations

IHC: identified using immunohistochemical
NCCN: National Comprehensive Cancer Network
ATP: adenosine triphosphate
TCGA: The Cancer Genome Atlas
TIMER: Tumor Immune Evaluation Resource
GO: gene ontology
CGGA: Chinese Glioma Genome Atlas